

UAV-BASED RADIO FREQUENCY SPECTRUM SENSING USING FPGA AND RADIO FREQUENCY MODULATION CLASSIFICATION.

M.Tech Thesis

By:

Tejas Rajuskar



**DEPARTMENT OF ASTRONOMY , ASTROPHYSICS AND SPACE
ENGINEERING**

INDIAN INSTITUTE OF TECHNOLOGY INDORE

May 28, 2025

UAV-BASED RADIO FREQUENCY SPECTRUM SENSING USING FPGA AND RADIO FREQUENCY MODULATION CLASSIFICATION

A THESIS

*Submitted in partial fulfillment of the
requirements for the award of the degree*

of

Master of Technology

by

Tejas Rajuskar



**DEPARTMENT OF ASTRONOMY , ASTROPHYSICS AND SPACE
ENGINEERING**

INDIAN INSTITUTE OF TECHNOLOGY INDORE

May 28, 2025




INDIAN INSTITUTE OF TECHNOLOGY INDORE

CANDIDATE'S DECLARATION

I hereby certify that the work which is being presented in the thesis entitled “**UAV-Based Radio Frequency Spectrum Sensing using FPGA and Radio Frequency Modulation Classification**” in the partial fulfillment of the requirements for the award of the degree of **MASTER OF TECHNOLOGY** and submitted in the **DEPARTMENT OF Astronomy, Astrophysics and Space Engineering, Indian Institute of Technology Indore**, is an authentic record of my own work carried out during the time period from August 2023 to May 2025 under the supervision of **Prof. Abhirup Datta**.

The matter presented in this thesis has not been submitted by me for the award of any other degree of this or any other institute.


16/05/2025

**Signature of the student with date
(Tejas Rajuskar)**

This is to certify that the above statement made by the candidate is correct to the best of my/our knowledge.

16-05-2025



Signature of the Supervisor of
M.Tech. thesis (with date)
(Prof. Abhirup Datta)

Tejas Rajuskar has successfully given his/her M.Tech. Oral Examination held on **6th May 2025** .



Signature(s) of Supervisor(s) of MTech thesis
Date: 16/05/2025



Convenor, DPGC
Date: 16/05/2025



Programme Coordinator, M.Tech.
Date: 16-05-2025



HoD, DAASE
Date:

ACKNOWLEDGEMENT

I would like to express my deepest gratitude to my supervisor, **Prof. Abhirup Datta**, for his invaluable support, guidance, and encouragement throughout this thesis. From the very beginning, he placed his trust in me and gave me the freedom to explore and learn independently, while always being there with thoughtful advice and clarity whenever I needed direction. Working under his supervision has been one of the most enriching experiences of my academic journey. His deep knowledge, research acumen, and humble nature have left a lasting impression on me. He not only guided me academically but also helped shape my perspective on how to approach problems with both curiosity and discipline. One of the most impactful contributions he made to my journey was providing me with the project idea and essential resources, which not only helped me grow technically but also played a major role in helping me land a job. The relevance and depth of the work we undertook together opened up opportunities for me professionally, and for that, I am especially grateful. His mentorship extended far beyond just thesis guidance—it helped pave a career path for me. I also deeply appreciate his patience and approachability. He always encouraged me to ask questions, however simple they might seem, and was never too busy to respond with kindness and insight. His consistent belief in my abilities gave me the confidence to move forward even during times of doubt. This thesis is not just the outcome of months of work, but also a reflection of the invaluable learning and mentorship I received under Prof. Abhirup Datta. I consider myself fortunate to have worked under his guidance, and I will always carry forward the lessons, values, and motivation he instilled in me. Thank you, sir, for being such a pivotal part of this journey.

I am also grateful to STARC Lab and its members for their invaluable assistance and collaboration. Special thanks to Harsha Tanti (PhD), Bhuvnesh Brawar (PhD) for their support. Their constructive criticism and thoughtful discussions helped refine my ideas and overcome numerous challenges during the project. I would also like to acknowledge my colleagues and classmates—Shubhi, Souradeep, Eeshan, Rajat—along with all my friends on campus, who have been a great source of motivation and support throughout my academic journey.

ABSTRACT

This thesis is divided in two stages. The first stage showcases a methodical implementation for a real-time RF emission acquisition, storage, and analysis system, useful for a variety of uses, including spectrum sensing, RF fingerprinting, commercial communication, electronic warfare, and more. The receiving antenna, low noise amplifiers, signal mixers, band-pass filters, and other components make up the analog front end of an RF signal acquisition chain. In order to process the continuous input RF signal from the front-end using digital computing devices such as a CPU (such as a Raspberry Pi SBC) and FPGA (such as a Xilinx ZCU-104), an ADC in the system backend transforms it into digital form. The Red Pitaya STEM Lab 125-10 serves as the main signal collection device in this project, which simulates an electronic warfare system and uses a small signal acquisition and recording system with a simple analog front-end. A Raspberry Pi 3B+ (Single Board Computer) receives the obtained samples for software-based signal processing and analysis. The Red Pitaya's RF input "IN1" has a 50 MHz LPF and a preset sampling rate of 125 MSPS. Strategic and commercial enterprises will employ the system, which consists of the Red Pitaya, Raspberry Pi, and antenna front-end, for remote data collecting applications using drones, unmanned vehicles, and other devices.

The second stage explores the amalgamation of Machine Learning Techniques and Radio Communications analysis methods already in place. Accurate classification of radio signals plays a vital role in numerous applications, ranging from wireless communication systems to spectrum monitoring. Traditionally, this task has depended heavily on manual feature engineering techniques such as the Fourier Transform, SIFT, and MFCC, which require domain expertise and extensive preprocessing. In recent years, however, machine learning—particularly advances in deep learning—has enabled more flexible and powerful solutions by allowing models to learn directly from raw data. This study explores a machine learning approach developed to address the limitations of earlier models, such as ResNet, which struggle with low signal-to-noise ratio (SNR) environments. The method described is designed to maintain strong classification performance regardless of noise level, eliminating the need for handcrafted features

or signal denoising. The method utilizes a hybrid model structure (Ensambled Model) for the same. Unlike traditional pipelines, the model processes raw signal inputs directly, adapting to both high and low SNR conditions. Extensive experiments demonstrate that our approach delivers superior results compared to prior methods, particularly in challenging, noisy scenarios.

Contents

List of Figures	IX
List of Tables	XI
1 Introduction	1
1.1 Background	1
1.1.1 Radio Frequency Signal Sensing	1
1.1.2 Radio Frequency Modulation Classification	3
1.2 Motivation	5
2 System Components Overview	6
2.1 Red Pitaya StemLab 125-10	6
2.2 Antenna Frontend	8
2.2.1 Donut Wideband Antenna	8
2.2.2 Transimpedance Amplifier	10
2.3 Data Processing Unit	11
2.3.1 Raspberry Pi 3B+	11
2.4 Radio Frequency Signal Source	13
2.4.1 ADF4351-PLL Frequency Synthesizer	13
3 Methodology	14
3.1 Radio Frequency Signal Sensing	14
3.1.1 System Block Design	14

3.1.2	System Setup	15
3.1.3	System Workflow	16
3.2	Radio Frequency Modulation Classification	18
3.2.1	Proposed Method	18
3.2.2	Dataset	19
3.2.3	Methodology for High SNR Classification Model (Modified ResNet)	21
3.2.4	Methodology for Low SNR Classification Model (Transformer)	25
4	Results	29
4.1	Radio Frequency Signal Sensing	29
4.2	Radio Frequency Modulation Classification	32
4.2.1	High SNR (Modified Residual Network)	32
4.2.2	Low SNR (Transformer Network)	33
4.2.3	Low SNR + High SNR (Ensembled Output from both Networks)	34
4.2.4	Comparison with Baseline ResNet Network	35
5	Project Conclusion	37
6	Future Work	38
	Bibliography	40

List of Figures

1.1	Resnet Model Performance vs Modulation Type	4
2.1	The Red Pitaya StemLab 125-10 Platform	7
2.2	Donut Wideband Antenna	9
2.3	S11 Parameter Measurement of Donut Antenna	10
2.4	Transimpedance Amplifier Circuit	11
2.5	Transimpedance Amplifier Package	11
2.6	RaspberryPi 3B+ Microprocessor Board	12
2.7	RF Signal Source ADF4351	13
3.1	RF Signal Capture Chain Block Diagram	15
3.2	RF Signal Capture Setup	15
3.3	LTC2185 16-Bit, 125Msps Low Power Dual ADCs	17
3.4	Proposed Hybrid Model Structure	19
3.5	Proposed Hybrid Model Expected Response	19
3.6	Radio Signal Samples From Dataset	20
3.7	A High SNR signal sample from the RADIOML 2018.01A dataset	21
3.8	A Low SNR signal sample from the RADIOML 2018.01A dataset	21
3.9	Skip Connection Feature in Residual Network	22
3.10	Skip Connection Feature in Residual Network	24
3.11	RNN working process	25
3.12	LSTM Structure	26

3.13 RNN Based Encoder and Transformer's Encoder	27
4.1 Synthetic Spectrum Plot for Signal Detection	29
4.2 Observed Spectrum Plot for 40MHz RF emission	30
4.3 Observed Spectrum Plot for Multiple Simultaneous RF emissions	31
4.4 Observed Spectrum Plot for 1.38MHz Unknown RF emission	32
4.5 Result for High SNR Model	33
4.6 Result for Low SNR Model	34
4.7 Ensembled Result of two Neural Networks	35
4.8 Comparison with Baseline ResNet Network	36

List of Tables

2.1	Red Pitaya StemLab 125-10 I/O Parameters	8
3.1	Optimizer: Stochastic Gradient Descent (Baseline model)	23
3.2	Optimizer: LazyAdam (Modified model)	23
3.3	Proposed Transformer Architecture (Optimizer: LazyAdam)	28
4.1	RF Sources with their Frequencies and Transmission Amplitudes	31
4.2	Probable RF Emission Sources for Signal detected at 1.35 to 1.5 MHz	32

Chapter 1

Introduction

1.1 Background

1.1.1 Radio Frequency Signal Sensing

This project operates in the domain of Electronic Warfare, Especially SIGINT and ELINT. *Signal Intelligence (SIGINT)* stands as a cornerstone in the realm of contemporary intelligence gathering, offering unparalleled insights into electronic communications and signals. This intelligence form has grown indispensable for national security, military operations, and law enforcement agencies worldwide. By intercepting and analyzing electronic signals, SIGINT provides critical information that helps identify and mitigate threats, track adversaries, and support strategic decision-making. To appreciate its significance in today's world, one must delve into its various applications, technological advancements, and notable examples from recent history (9).

Signal Intelligence encompasses the interception and analysis of signals such as communications (**COMINT**) and electronic signals not intended for communication (**ELINT**). COMINT involves monitoring voice and data transmissions between individuals or organizations, providing valuable insights into their plans and activities. ELINT, on the other hand, focuses on electronic emissions from radar, navigation, and other non-communication sources, offering information on the capabilities and locations of various electronic systems (9).

The technological landscape has evolved significantly, bolstering SIGINT capabilities. Ad-

vances in digital communications, encryption, and data transmission have posed challenges to SIGINT operations, necessitating the development of more sophisticated interception and decryption techniques.

- **Drones and Unmanned Aerial Vehicles (UAVs):** Drones equipped with SIGINT payloads can conduct surveillance operations over hostile territories, intercepting communications and electronic signals with high precision. Their ability to loiter over areas for extended periods enhances their effectiveness in gathering intelligence.
- **Satellites:** Satellite-based SIGINT systems provide global coverage, enabling the interception of signals from virtually anywhere on Earth. These systems are crucial for monitoring high-frequency communications and electronic emissions from military installations, ships, and aircraft(13).
- **Cyber-SIGINT:** With the proliferation of digital communications, cyber-SIGINT has become a critical component. It involves monitoring internet traffic, emails, and other forms of digital communication to detect and prevent cyber threats. Techniques such as deep packet inspection and metadata analysis play a significant role in cyber-SIGINT operations.

The importance of SIGINT in today's security landscape cannot be overstated. It provides a strategic advantage by offering early warning of potential threats, supporting military operations, and enhancing law enforcement capabilities.

- **Counterterrorism:** SIGINT has been instrumental in counterterrorism operations, helping to identify and neutralize terrorist threats. A notable example is the operation that led to the elimination of Osama bin Laden. SIGINT played a crucial role in tracking his communications and movements, ultimately leading to his location and capture.
- **Military Operations:** In military operations, SIGINT provides real-time battlefield intelligence, enabling commanders to make informed decisions. During the Gulf War,

SIGINT was used extensively to intercept Iraqi communications, providing valuable information on troop movements and strategic plans.

- **Cybersecurity:** The rise of cyber threats has made SIGINT an essential tool in cybersecurity. It helps detect and prevent cyberattacks on critical infrastructure, such as power grids, financial systems, and government networks. The detection of the SolarWinds cyberattack in 2020, where Russian hackers infiltrated numerous U.S. government agencies, underscored the importance of SIGINT in identifying and mitigating cyber threats.
- **Law Enforcement:** SIGINT supports law enforcement agencies in combating organized crime, drug trafficking, and human trafficking. By intercepting communications between criminal networks, law enforcement agencies can gather evidence, track suspects, and dismantle criminal operations.

1.1.2 Radio Frequency Modulation Classification

Swift and autonomous comprehension of radio spectrum is crucial for contemporary applications including spectrum interference monitoring, radio fault detection, dynamic spectrum access, opportunistic networking, and diverse regulatory and defence activities. Military communications predominantly depend on wireless technologies, wherein radio signal surveillance can yield essential insights into enemy activities, encompassing detection, location, and signal identification. This work was historically executed manually by skilled operators employing auditory recognition methods.

Historically, the classification of radio signals and recognition of modulation were accomplished using manually designed feature extraction specific to particular signal categories. These characteristics were employed to delineate decision boundaries either analytically or statistically inside low-dimensional areas. The human interpretation of radio signals is fundamentally constrained by the difficulty of distinguishing signals through visual analysis alone. Thus, feature extraction becomes a necessary task prior to execution of classification. Two traditional methodologies have been utilized. The initial approach employs statistical modulation

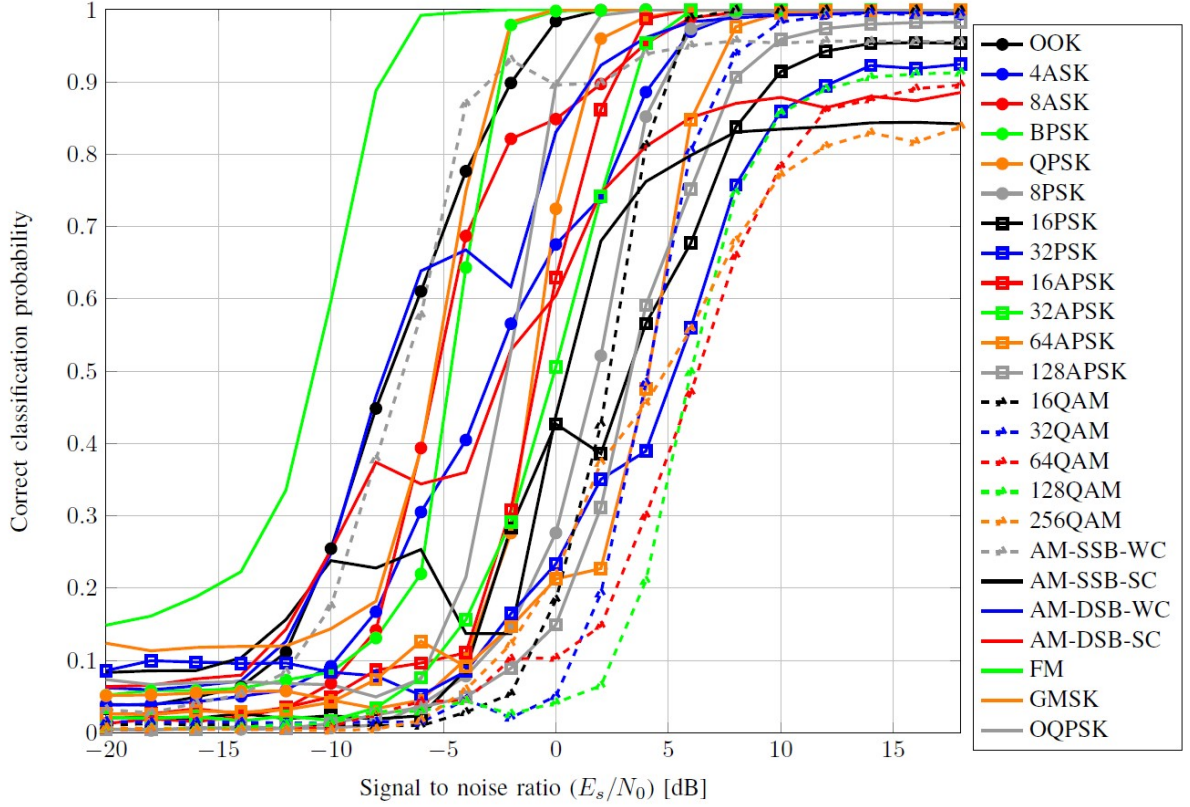


Figure 1.1: Resnet Model Performance vs Modulation Type
(1)

characteristics, extracting attributes such as carrier structure, symbol timing, and symbol configuration, which are subsequently processed by machine learning models for categorization. This strategy is successful but depends significantly on comprehensive information; absent parameters may impair results. The alternative method entails the development of stochastic radio channel models. This method, while simplifying feature modelling, necessitates predetermined models and does not accommodate raw signal input for direct categorization.

Conversely, deep learning has transformed pattern recognition, especially in computer vision, by obviating the necessity for manually produced features. This paradigm change has encompassed radio signal classification. In 2018, researchers exhibited the efficacy of deep learning, particularly ResNet, in identifying radio signals, attaining approximately 94% accuracy at elevated signal-to-noise ratios (SNRs). The approach functioned directly on raw data, eliminating the necessity for feature engineering, denoising, or preprocessing, hence underscoring the robustness and generalization capacity of deep neural networks.

These developments suggest that deep learning provides a robust and scalable alternative to conventional approaches. Its capacity to autonomously acquire discriminative features from raw radio data establishes it as the new benchmark for radio signal classification, particularly in contexts where prior information is scarce or insufficient.

1.2 Motivation

In recent years, we have seen a massive rise in the use of drones and electronic warfare techniques deployed during wartime. Often, they have been used as a combined system and have excelled as such. With keen interest in the world of defence and defence technologies, the use of unique technologies has sparked an interest to replicate some of them for indigenous use cases. The Ukraine war has indeed been a showcase of modern warfare, with drones and electronic warfare playing pivotal roles. Here are some key insights about use of drones in the Ukraine War:

1. **Versatility and Adaptability:** Drones have been used for a variety of purposes, from reconnaissance to direct attacks. Both sides have employed drones to monitor enemy movements, direct artillery strikes and even deliver explosives.

2. **Cost-Effective Warfare:** Commercial drones, like the DJI Mavic series, have been modified for military use. These low-cost drones have allowed smaller forces to challenge larger, more traditional military powers.

3. **Innovation in Tactics:** Ukrainian forces have used drones to drop grenades and improvised explosives on enemy positions. This has demonstrated the adaptability of civilian technology for military applications.

4. **Game Changers:** Drones have levelled the playing field, enabling both sides to conduct precision strikes and gather real-time intelligence without risking human lives

Similar trends have been seen in conflicts in Israel and Indo-China border Regions. This generated a need to dive into the field of Electronic Warfare and develop a Product or technique to assist the end users.

Chapter 2

System Components Overview

This chapter provides a comprehensive overview of the fundamental components that constitute a system. Understanding each element—ranging from hardware and software modules to interfaces and communication protocols—is essential for grasping the overall functionality and behavior of complex systems. By examining how these components interact and integrate, this chapter sets the foundation for analyzing system performance, reliability, and scalability in subsequent sections.

2.1 Red Pitaya StemLab 125-10

The Red Pitaya STEMLab 125-10 is a tiny, open-source measurement and control platform that integrates a dual-core ARM Cortex-A9 processor with a Xilinx Zynq 7010 FPGA. It facilitates high-speed analog and digital I/O with 125 MS/s ADCs and DACs, rendering it exceptionally appropriate for signal acquisition, production, and processing activities. Its integrated characteristics enable it to emulate the functions of conventional laboratory instruments, including oscilloscopes, spectrum analyzers, and signal generators, in a portable format.

We selected the Red Pitaya STEMLab 125-10 as our RF sensing platform because of its real-time signal processing capabilities, extensive analog bandwidth, and adaptable programmability. These attributes render it optimal for the detection, analysis, and characterization of RF

signals in dynamic situations, facilitating precise spectrum monitoring and anomaly detection within a small, economical configuration.

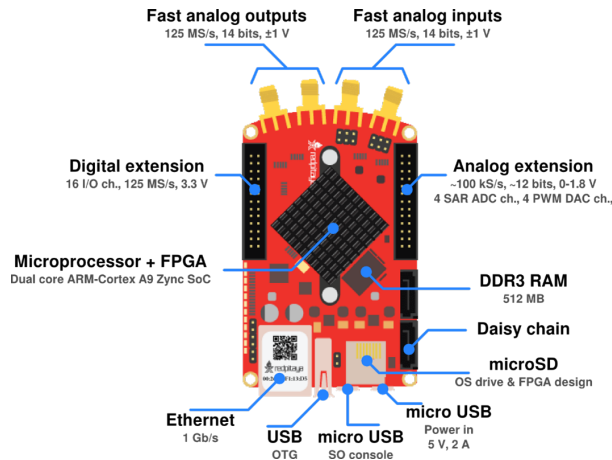


Figure 2.1: The Red Pitaya StemLab 125-10 Platform

The input/output (I/O) parameters of the Red Pitaya STEMLab 125-10 are crucial for determining its suitability for various RF sensing and signal processing applications:

- **Sample Rate (125 MSPS):** A high sampling rate allows accurate digitization of high-frequency signals without aliasing, making it essential for time-domain analysis and frequency-domain measurements.
- **ADC Resolution (10-bit):** This defines the precision of the analog-to-digital conversion. A 10-bit resolution provides a balance between dynamic range and data processing requirements, suitable for many mid-resolution RF applications.
- **Full Scale Voltage Range (± 1 V / ± 20 V):** The selectable voltage range on the input ports enhances versatility, allowing the platform to interface with both low-level and high-voltage signals without additional conditioning.
- **Bandwidth (DC–50 MHz input, DC–40 MHz output):** The wide analog bandwidth supports a broad range of signal types, from baseband to RF, enabling analysis of low to mid-frequency RF signals with high fidelity.
- **Impedance (1 M Ω input, 50 Ω output):** High input impedance ensures minimal loading

Table 2.1: Red Pitaya StemLab 125-10 I/O Parameters

Parameters	Input Ports	Output Ports
Sample Rate	125 MSPS	125 MSPS
ADC resolution	10-bit	10-bit
Full Scale Voltage Range	+1V / +20V	+1V
BW	DC-50 MHz	DC-40 MHz
Impedance	Input: $1M\Omega$	Load Impedance: 50Ω

on the signal source, while a standard 50Ω output impedance ensures compatibility with RF test equipment and transmission lines.

Together, these parameters define the performance envelope of the STEMLab 125-10, ensuring accurate signal acquisition, processing, and transmission in portable, real-time RF sensing systems.

2.2 Antenna Frontend

2.2.1 Donut Wideband Antenna

The antenna frontend plays a critical role in any RF sensing system by capturing electromagnetic signals from the surrounding environment. In this setup, we employ the Donut Wideband Antenna, which operates efficiently across a broad frequency range of 10 kHz to 180 MHz. This antenna is specifically designed to support wideband reception, making it suitable for low-frequency RF monitoring, signal intelligence, and spectrum sensing applications.

Its omnidirectional design ensures uniform sensitivity to signals arriving from all directions, while its wide operational bandwidth allows the system to detect a diverse range of RF sources. By integrating this antenna with the Red Pitaya STEMLab 125-10 platform, we enable effective acquisition and analysis of RF signals across a wide frequency spectrum, forming a robust front-end for versatile sensing and monitoring tasks.

This antenna has been specifically selected for our portable setup due to its compact, lightweight, and rugged design, which ensures ease of deployment in field conditions without

compromising performance. Its omnidirectional reception pattern and consistent gain across the band further enhance its utility in dynamic environments, making it ideal for mobile RF sensing applications where flexibility, reliability, and broad frequency coverage are essential.

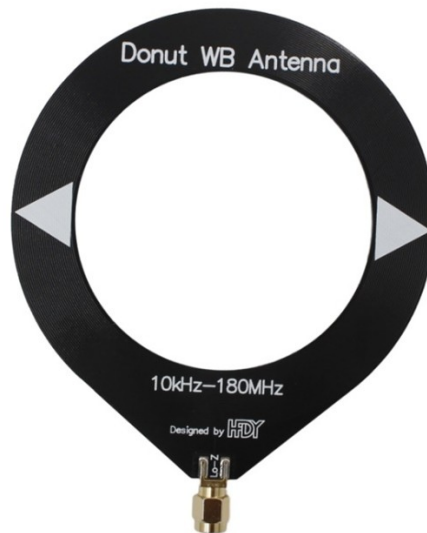


Figure 2.2: Donut Wideband Antenna

The ***S11 parameter***, also known as the reflection coefficient or return loss, is a key metric in antenna characterization. It represents the amount of power reflected back from the antenna input port relative to the power supplied, typically expressed in decibels (dB). An S11 value of 0 dB indicates total reflection (poor matching), while values below -10 dB are generally considered acceptable, indicating that at least 90% of the power is being transmitted into the antenna.

In the provided S11 measurement plot for the Donut Wideband Antenna (10 kHz to 180 MHz), the curve shows how well the antenna is matched across its operating frequency range. Observing low S11 values (more negative) across a wide bandwidth indicates good impedance matching, which is critical for efficient power transfer, minimal signal loss, and optimal antenna performance. These characteristics confirm that the antenna is well-suited for broadband RF sensing in our portable setup.

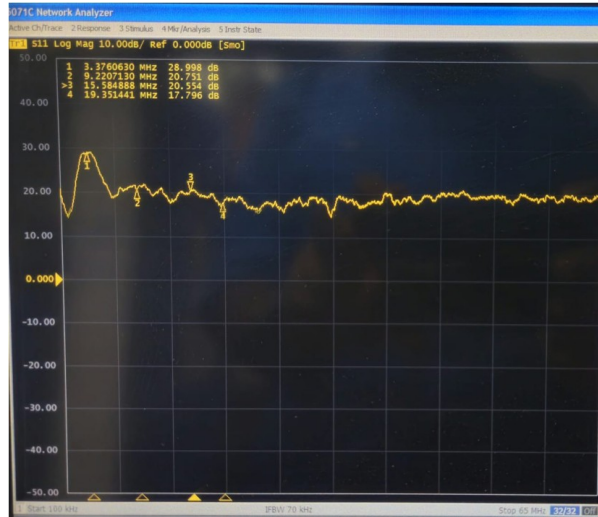


Figure 2.3: S11 Parameter Measurement of Donut Antenna

2.2.2 Transimpedance Amplifier

A transimpedance amplifier (TIA) is a critical circuit element used to convert low-level input currents into measurable voltage signals, making it essential in systems where signal strength is weak or prone to noise. In our RF sensing setup, the TIA is positioned between the Donut Wideband Antenna and the signal processing unit to enhance sensitivity and signal integrity. The transimpedance amplifier (TIA) used in our portable RF sensing system offers a compact yet efficient design tailored for low-frequency signal amplification. Operating over a wide frequency range of **10 kHz to 180 MHz**, it is well-matched with the Donut Wideband Antenna and capable of processing a broad spectrum of RF signals with stability and precision.

A key advantage of this TIA is its **built-in 600 mAh lithium battery**, which enables **up to 20 hours of continuous use**, making it ideal for field and mobile deployments. The device charges via a **Type-C interface** at **5V/1A**, reaching full capacity in **approximately 4 hours**. Its intuitive LED indicators—**red for charging** and **green when fully charged**—enhance usability.

Weighing only **56 grams**, the amplifier is exceptionally lightweight and portable. These features collectively ensure that the TIA is not only capable in terms of signal amplification but also optimized for extended use in remote or mobile RF sensing setups, aligning perfectly with the design goals of our compact and energy-efficient system. When the Donut Wideband

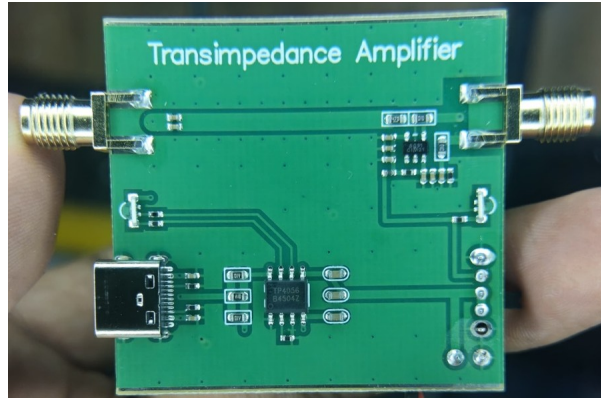


Figure 2.4: Transimpedance Amplifier Circuit



Figure 2.5: Transimpedance Amplifier Package

Antenna captures weak RF signals—especially in the low-frequency range—it induces small currents. The TIA amplifies these currents and converts them into voltage signals that are better suited for digitization and analysis by the Red Pitaya STEMLab 125-10 platform. This amplification not only improves the signal-to-noise ratio but also ensures accurate and reliable RF measurements, thereby enabling effective sensing in portable and low-power environments.

2.3 Data Processing Unit

2.3.1 Raspberry Pi 3B+

The Raspberry Pi 3+ is a compact, affordable, and powerful single-board computer that plays a central role in our RF sensing system. Equipped with a 1.4 GHz quad-core ARM Cortex-A53 processor and built-in Wi-Fi and Bluetooth connectivity, it serves as the primary processing unit for data handling, control, and communication tasks.

In this project, the Raspberry Pi 3+ is crucial for processing the digitized signals received

from the Red Pitaya STEMLab 125-10. It manages data logging, visualization, and remote access functionalities, making the system highly autonomous and user-friendly. Its low power consumption and GPIO flexibility also support seamless integration with other modules, such as the transimpedance amplifier and power management units. Overall, the Raspberry Pi 3+ enables real-time data processing and system control in a compact and portable platform, aligning perfectly with the design objectives of our field-deployable RF sensing setup.

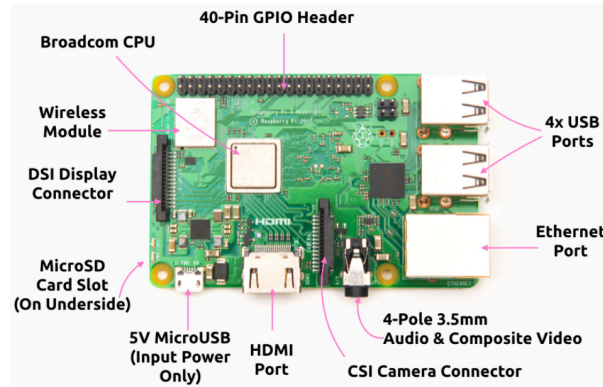


Figure 2.6: RaspberryPi 3B+ Microprocessor Board

To enable real-time data acquisition and analysis in our RF sensing setup, we utilized Python on the Raspberry Pi 3+ for system control and signal processing. Python's simplicity and extensive library support made it ideal for interfacing with the Red Pitaya STEMLab 125-10, handling communication protocols, and automating data logging and visualization tasks.

Custom Python scripts were developed to initiate signal acquisition, read S-parameter or voltage data, and process it in real time. The scripts also included logic for triggering, threshold monitoring, and saving critical signal events for offline analysis. This flexible and lightweight approach allowed seamless integration of hardware and software components, enabling efficient and portable testing in dynamic field environments.

2.4 Radio Frequency Signal Source

2.4.1 ADF4351-PLL Frequency Synthesizer

The ADF4351-PLL is a highly versatile RF signal generator module that utilizes a phase-locked loop (PLL) synthesizer to generate stable and tunable frequencies ranging from 35 MHz to 4.4 GHz. In our project, the ADF4351 serves as a critical RF signal source, enabling the controlled generation of test signals for system calibration, validation, and performance analysis. Its abil-

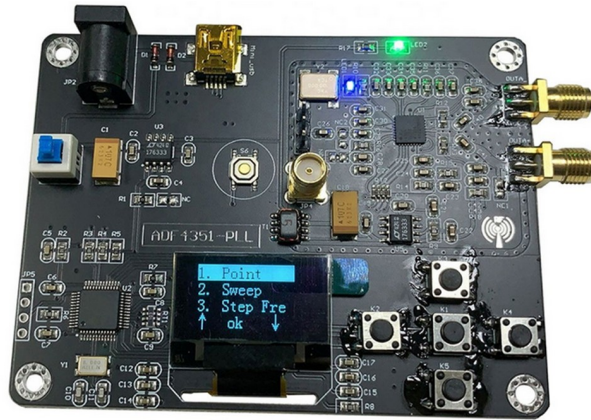


Figure 2.7: RF Signal Source ADF4351

ity to produce a wide range of precise frequencies allows us to simulate various RF scenarios and test the sensitivity, linearity, and response of the sensing system under controlled conditions. The ADF4351's compact size, programmable interface, and low phase noise make it an ideal choice for integration with our portable setup. By using this module, we ensure consistent and repeatable testing conditions, which are essential for verifying the accuracy and reliability of the RF sensing platform in both laboratory and field environments.

To assess the performance and robustness of our RF sensing system, we used multiple ADF4351-PLL modules to generate real-time RF signals at varying frequencies. This created a dynamic RF environment to test the system's ability to detect, distinguish, and process overlapping or rapidly changing inputs. The setup was key for stress-testing and validating real-time responsiveness in complex scenarios.

Chapter 3

Methodology

3.1 Radio Frequency Signal Sensing

3.1.1 System Block Design

The RF signal chain illustrated below represents the complete flow of signal acquisition, processing, and analysis in our portable sensing system. It begins with a **transmitter antenna** generating RF signals, which are captured by a **wideband receiving antenna** (Donut antenna). These signals are then fed into the **Red Pitaya STEMLab 125**, which acts as a high-speed digitizer and interface platform for capturing and forwarding the signals.

Communication between the Red Pitaya and the **Raspberry Pi 3B+** is established via **SCPI (Standard Commands for Programmable Instruments)** over a network interface, enabling seamless control and data transfer. The Raspberry Pi handles real-time **signal processing**, including FFT computation, visualization, and event-based analysis, all implemented through Python.

This tightly integrated signal chain enables robust and flexible RF spectrum sensing. It combines the advantages of low-power embedded platforms with high-resolution data acquisition, making it ideal for mobile or field-based RF monitoring applications.

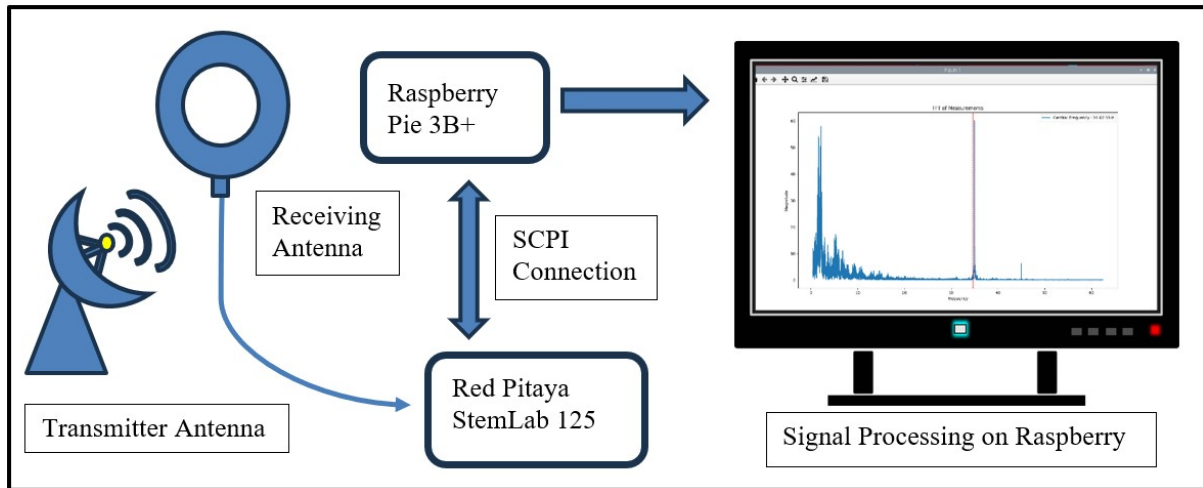


Figure 3.1: RF Signal Capture Chain Block Diagram

3.1.2 System Setup

The figure below shows the complete hardware assembly of our portable RF signal capture system. At the core of the setup is the **Donut Wideband Antenna** (10 kHz–180 MHz), which is responsible for receiving ambient RF signals across a broad frequency range. This antenna is connected to a compact **Transimpedance Amplifier (TIA)**, which amplifies weak incoming signals and converts them from current to voltage for accurate analysis.

The output of the TIA feeds into the **Red Pitaya STEMLab 125-10** board, which serves as the data acquisition unit. It digitizes the amplified RF signals using its high-speed ADC and forwards the data to the **Raspberry Pi 3B+**, shown housed in a red case. The Raspberry Pi handles the control and processing tasks, communicating with Red Pitaya via SCPI commands and executing real-time signal analysis using Python-based scripts.



Figure 3.2: RF Signal Capture Setup

3.1.3 System Workflow

- **Radio Frequency Frequency Reception:** The RF signal within the bandwidth of 10 KHz - 65 MHz is received by the Donut antenna as current. The Transimpedance amplifier lowers the impedance of antenna for the observation frequency window and allows a wide frequency response along with reducing noise and interference. We simulate synthetic signals using the RF Signal Source between 35MHz and 65 MHz with amplitudes up to +5dB and transmit using a Dipole Antenna.
- **Radio Frequency Capture:** The RF signal is then applied via SMA Cable to the IN1 input of Red Pitaya StemLab 125-10. This RF Signal Input is fed through **Channel-1** to the 10-Bit ADC (**LTC2185**) in Red Pitaya, which then converts analog voltage values to digital ones. The system generates 16,358 data points for each sampling, giving a complete sweep of observation frequency window. The Red pitaya stores these values in a buffer for transfer to the Raspberry pi Single Board Computer for further signal processing.
- **Radio Frequency Processing:** The raspberry pi connects to the Red pitaya through the Ethernet via SCPI (i.e. Standard Commands for Programmable Instruments), which defines a syntax and text-based commands for controlling programmable test and measurement instruments such as Red pitaya StemLab 125-10.

Furthermore, we use python 3 as the scripting language for the signal processing part. With the sampling frequency of the red pitaya set at 125 Mega samples per second, we perform read through the data points and utilize the **FFT** (Fast Fourier Transform) operation in **SciPy** python library, whose mathematical representation is given as;

$$X(k) = \frac{1}{N} \sum_{n=0}^{N-1} x(n) \cdot e^{-j\frac{2\pi}{N}kn}$$

The Fast Fourier Transform (FFT) is an efficient algorithm used to compute the Discrete Fourier Transform (DFT) of a sequence. It transforms a signal from the time domain into

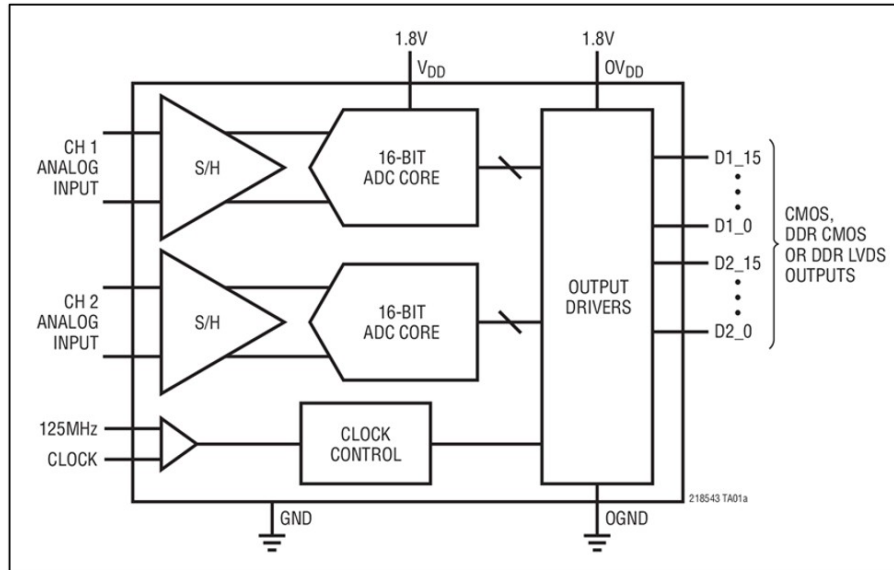


Figure 3.3: **LTC2185** 16-Bit, 125Msps Low Power Dual ADCs

the frequency domain, revealing the different frequency components present in the signal. It speeds up the computation of the Discrete Fourier Transform (DFT) by breaking the problem into smaller parts and using symmetry and periodicity properties of complex exponentials. . This is particularly useful in signal processing, image analysis, and data compression. By significantly reducing the computational complexity compared to directly calculating the DFT, the FFT enables real-time analysis of signals in various applications such as audio processing, telecommunications, and scientific measurements. Generally, the basic computations for such process analyzing signals include converting from a two-sided power spectrum to a single-sided power spectrum, adjusting frequency resolution and graphing the spectrum, using the FFT, and converting power and amplitude into logarithmic units.

Finally using the Matplotlib library, we plot the “FFT Amplitude against Frequency in MHz”, the plot is a continuous sweep which updates after every second, signalling the transfer of recorded data from red pitaya’s buffer to the raspberry pi for storage and processing.

3.2 Radio Frequency Modulation Classification

3.2.1 Proposed Method

Prior studies with ResNet achieved commendable accuracy in classifying ideal signals with minimal noise. However, ResNet has suboptimal performance when categorizing signals characterized by high noise levels. In practical applications, we cannot consistently expect to get an ideal signal characterized by low noise; we frequently encounter signals with significant noise levels. Consequently, our objectives will concentrate on the classification of signals in both low and high signal-to-noise ratio (SNR) conditions. Below section summarizes our project objectives:

Our objective is to enhance accuracy in low SNR signals without compromising accuracy in high SNR signals. This will demonstrate that our model is resilient to noisy signal modulation. Consequently, our technique could be applied in real-world conditions when an ideal, noise-free signal is not consistently available. We will develop a novel deep learning architecture and aim to achieve outcomes in accuracy that are comparable to or surpass the state of the art.

Our deep learning approach will utilize the RAW data directly as input, as preprocessing and denoising require distinct methods depending on the kind of signal. Consequently, in certain instances, we were unable to consistently utilize the preprocessed signal as our input.

Our suggested method employs two neural network models: one optimized for predicting signals with high signal-to-noise ratios (SNR) and the other for predicting signals with low SNR. For high SNR models, we will employ a Residual Network similar to our baseline approach, implementing modifications and adjustments to enhance its accuracy. For low SNR models, we will employ a transformer neural network, a type of time series neural network capable of predicting complex data, such as signals with a low SNR rate. After inputting our signal into two models, we will ensemble by selecting the output that yields the maximum accuracy from the two models.

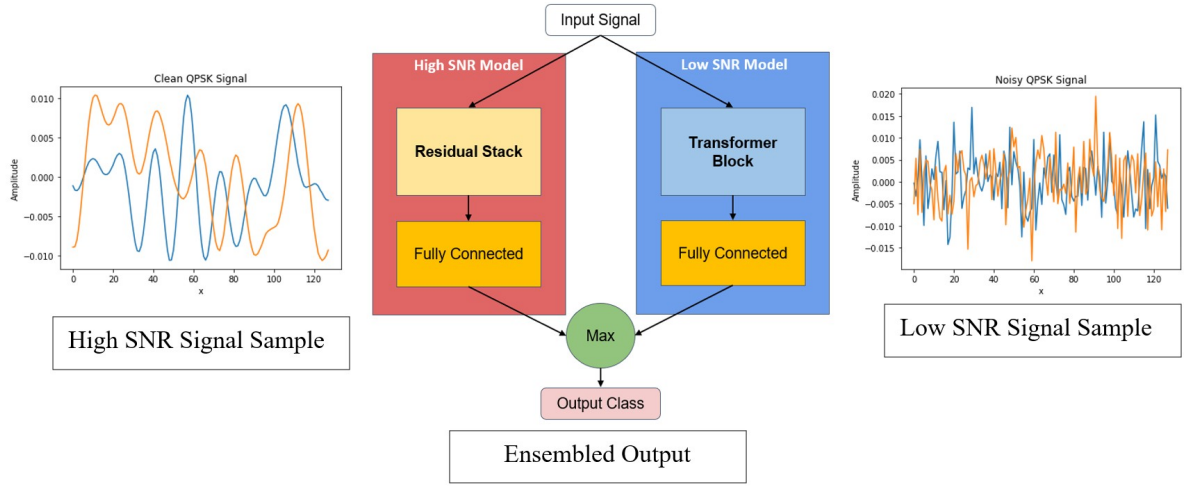


Figure 3.4: Proposed Hybrid Model Structure

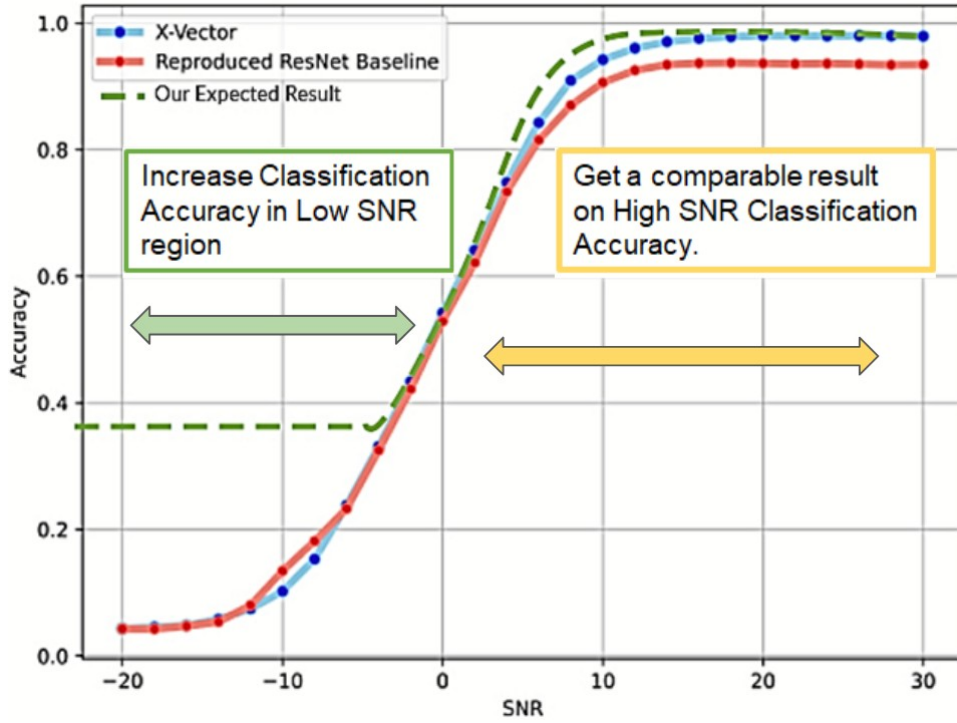


Figure 3.5: Proposed Hybrid Model Expected Response

3.2.2 Dataset

We utilize a dataset from DeepSig (RadioML 2018) that encompasses various types of communication signals. This dataset is pretty large (18GB) with consists of 24 types of signal modulation such as 32PSK, 16APSK, 32QAM, FM, GMSK, 32APSK, OQPSK, 8ASK, BPSK, 8PSK, AM-SSB-SC, 4ASK, 16PSK, 64APSK, 128QAM, 128APSK, AM-DSB-SC, AM-SSB-WC, 64QAM, QPSK, 256QAM, AM-DSB-WC, OOK, and 16QAM (1). This dataset has both

pristine signals and noisy signals. Signals are rarely in an ideal state; thus, we cannot directly replicate a pristine signal for classification purposes, as a model based solely on a clean signal will struggle to accurately identify signals encountered in everyday life. We must analyze the datasets and pick from them, utilizing the noisy signal to obtain representations of the signal under both low and high SNR situations. Certain prior methodologies remain inadequate for classifying signals in low signal-to-noise ratio (SNR) conditions, indicating that increased noise levels may lead to classification failures by the model. Utilizing advanced computer vision technology, we will enhance our processes, enabling the classification of high-noise signals without sacrificing accuracy for low-noise signals. Below are some of the signals that a machine will be able to differentiate.

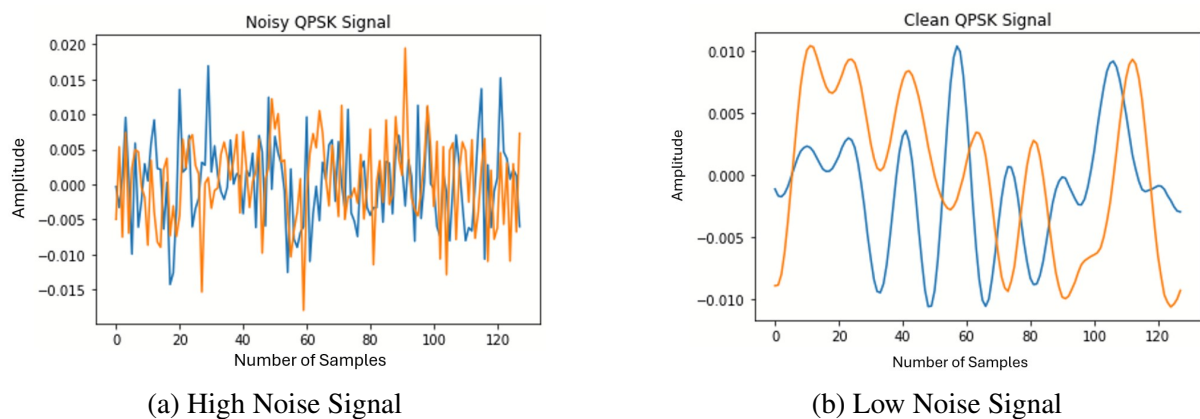


Figure 3.6: Radio Signal Samples From Dataset

Signal-to-Noise Ratio (SNR) is a key metric in communication and sensing systems that measures the strength of a signal relative to background noise. A **high SNR signal** indicates that the desired signal significantly exceeds the noise level, resulting in clear, easily detectable, and accurate data. Such signals are ideal for reliable processing and interpretation, as they maintain signal integrity even in complex environments.

In contrast, a **low SNR signal** occurs when the signal strength is comparable to or weaker than the surrounding noise. This makes detection and analysis challenging, often requiring advanced filtering, amplification, or signal enhancement techniques to recover meaningful information. In RF sensing applications, handling low SNR signals effectively is crucial, as real-world environments often contain interference, attenuation, or weak transmissions that

can degrade measurement accuracy.

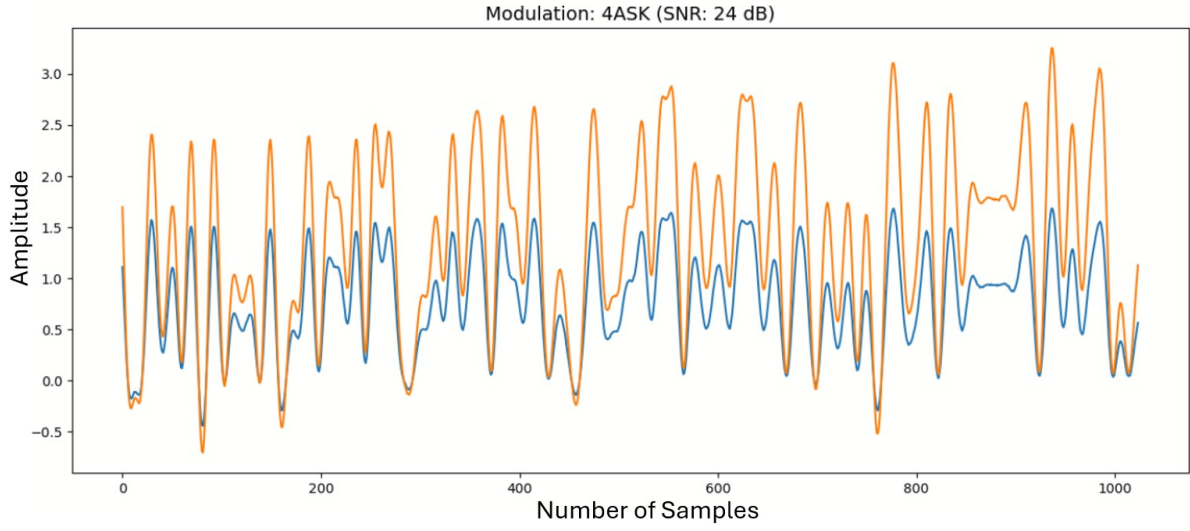


Figure 3.7: A High SNR signal sample from the RADIOML 2018.01A dataset

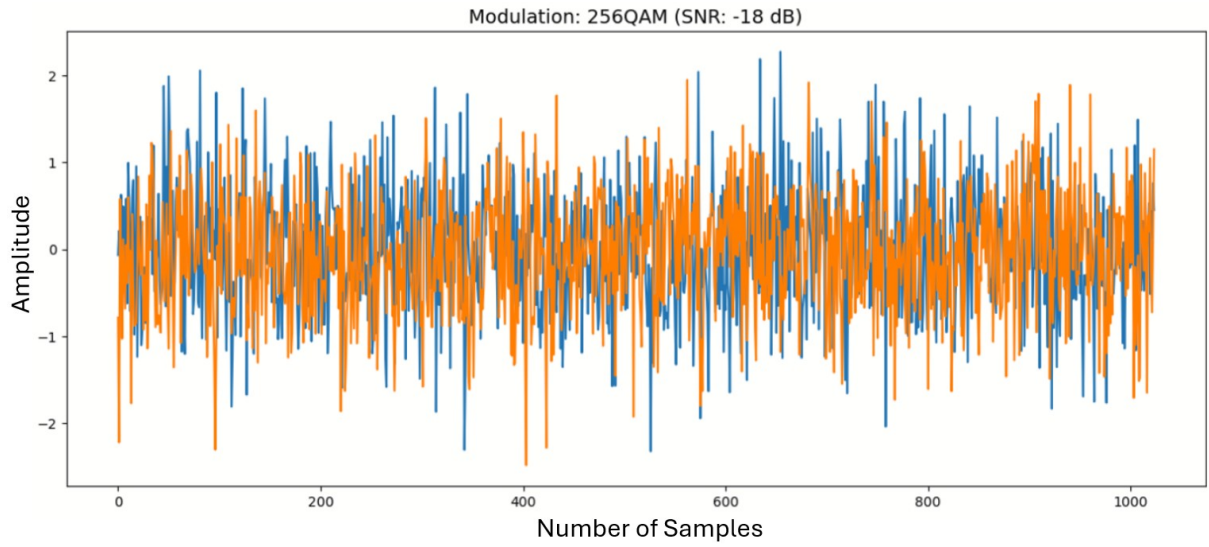


Figure 3.8: A Low SNR signal sample from the RADIOML 2018.01A dataset

3.2.3 Methodology for High SNR Classification Model (Modified ResNet)

We will first discuss the advantages of residual networks before outlining our methodology. Deep neural networks have advanced recently, with state-of-the-art architectures varying from numerous layers, such as AlexNet, to over one hundred layers. One of the main advantages of an exceptionally deep neural network is its capacity to represent detailed complex operations. A significant impediment to training them is that fading gradients in very deep networks often

result in a loss signal that rapidly approaches zero, rendering gradient descent exceedingly inefficient. Specifically, at each stage of grade descent — that is, as we backpropagate from the final subcaste to the initial subcaste — we are multiplying by the weight matrix. A significant number of proliferations results in minor slants; hence, the grade can rapidly decline exponentially to zero (or, in rare instances, increase exponentially and "explode" to attain exceedingly large values).

Standard networks refer to conventional architectures such as VGG-16. After thousands of cycles, the training error for a 56-layer network was lower than that of a 20-layer network in standard architectures as the number of layers climbed from 20 to 56 (as illustrated below). The training error was more pronounced in a 56-layer network compared to a 20-layer network, even after thousands of iterations in standard networks, as the number of layers increased from 20 to 56 (as illustrated below).

Declination is evident when deeper networks are appropriate for initiating clustering; delicacy becomes imbued, which may be unexpected, and concurrently diminishes rapidly as network depth escalates. The model's performance is declining due to the utilization of deeper networks. This issue is addressed in a Microsoft Research article through the use of a Deep Residual architecture.

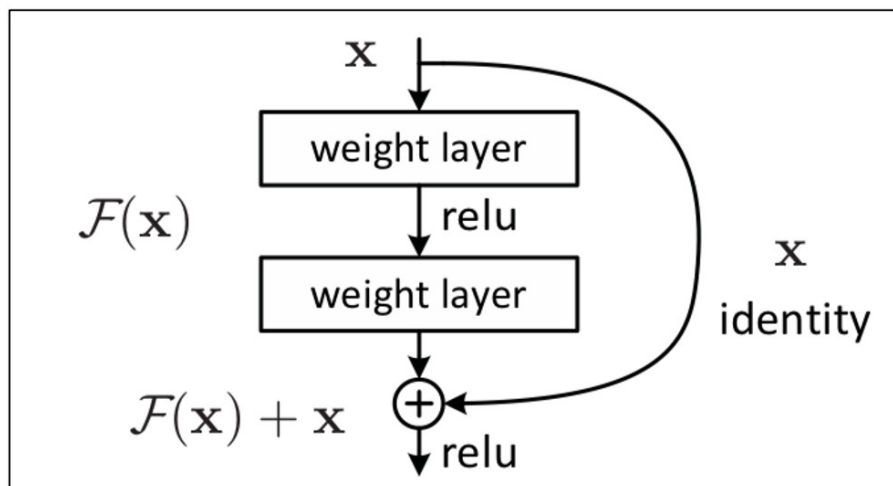


Figure 3.9: Skip Connection Feature in Residual Network

In essence, information is transmitted more efficiently from one subcaste to the subsequent subcaste by circumventing data through standard CNN influx, incorporating a pathway or skip

connection that facilitates data flow. Remove two from the remaining block, first. Incorporating additional layers will not impair the model’s performance, as regularization will disregard any ineffective layers. Secondly, if the redundant or new layers prove beneficial, the weights or kernels of these layers will be non-zero due to regularization, hence enhancing model performance. Consequently, it is guaranteed that the model’s performance will not decline; rather, it may slightly improve by incorporating additional layers due to the "skip connection" and "residual connection." One can create a rather profound network by stacking these ResNet units sequentially. Furthermore, the inclusion of ResNet blocks with a pathway facilitates the ability of one of the blocks to acquire an identity function effortlessly. Consequently, one can incorporate superfluous ResNet blocks with minimal risk of impacting training set performance.

Our conditioning employs a profoundly intricate neural network as we aim to classify 24 distinct sorts of signals that represent a complex function. Employing a shallow neural network will not resolve the issue; therefore, we must tackle the problem with a somewhat deep neural network.

Table 3.1: Optimizer: Stochastic Gradient Descent (Baseline model)

Layer	Output Dimension
Input	2×1024
Residual Stack	32×512
Residual Stack	32×256
Residual Stack	32×128
Residual Stack	32×64
Residual Stack	32×32
Residual Stack	32×16
FC/SeLU-Alpha Dropout	128
FC/SeLU-Alpha Dropout	128
FC/Softmax	24

Table 3.2: Optimizer: LazyAdam (Modified model)

Layer	Output Dimension
Input	2×1024
Residual Stack	32×512
Residual Stack	32×256
Residual Stack	64×128
Residual Stack	64×64
Residual Stack	32×32
Residual Stack	32×16
FC/SeLU-Alpha Dropout	128
FC/SeLU-Alpha Dropout	128
FC/Softmax	24

We apply advancements to the batch to enhance training effectiveness and accuracy factor. We supplanted the optimizer from Stochastic Gradient Descent (SGD) to the advanced optimizer known as LazyAdam. **LazyAdam** is a modified iteration of the most used Adam op-

timizer function that manages small updates with further enhanced results. The original Adam algorithm uses a combination of two moving-average accumulators for each trainable variable, which are also streamlined at each replication of the process(15). This class facilitates more effective operation of grade updates for meagre variables. It simply updates moving-average accumulators for meagre variable indicators present in the current batch, rather than for all indicators. In comparison to the classic Adam optimizer, it can significantly enhance model training outcomes for some operations. We also modify the number of pollutants in the third and fourth residual network heaps from the count of 32 to 64. We later exclude the final two residual heaps to enhance the training split, while contemporaneously drawing those factors to help inordinate information loss due to the skip connections within the residual network.

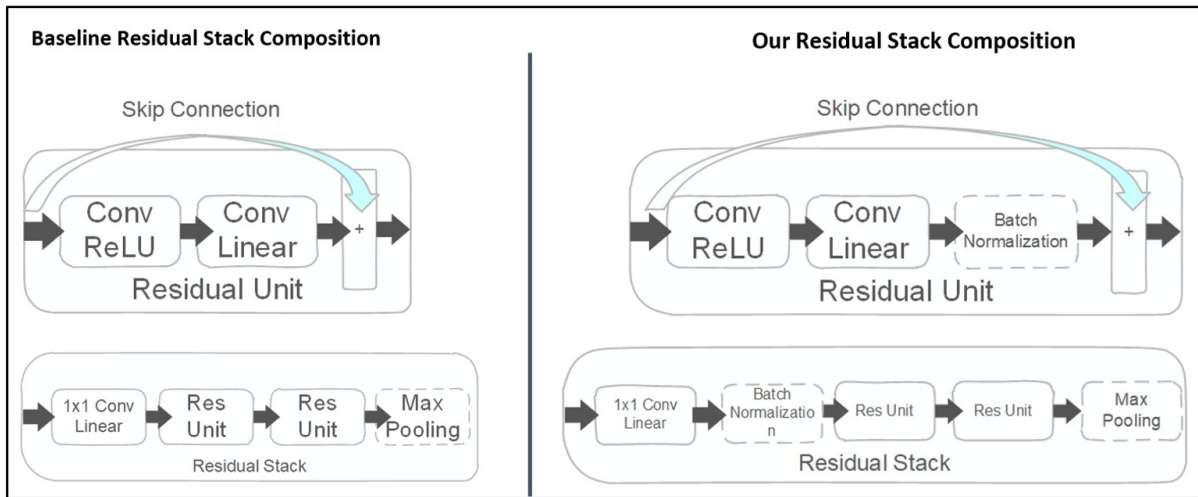


Figure 3.10: Skip Connection Feature in Residual Network

In addition to altering the neural network architecture depicted in the image over, we also acclimate the composition of the residual stack. We incorporated batch normalization within the residual unit, whereas the previous batch didn't use batch normalization for their residual network. Batch normalization is also used following the 1x1 convolutional direct layer within the residual stack.

Batch normalization is a method employed in the training of deep neural networks that normalizes the inputs to a layer for each mini batch. This stabilizes the learning process and significantly decreases the number of training epochs needed for deep network training(11). Batch normalization mitigates the extent of covariance shift in hidden unit values; for instance,

we train our model exclusively on photos of red flowers. Consequently, if we attempt to apply this network to data featuring differently coloured flowers, it is evident that we would not perform adequately. Batch normalization will address this issue.

Two insights from batch normalization are that it permits the use of elevated learning rates, as it ensures that no activation becomes excessively high or low. It mitigates overfitting because to its marginal regularization effect. Analogous to residual stacking, it introduces noise to the activations of each concealed layer. Consequently, the implementation of batch normalization will reduce the necessity for a substantial residual stack, which is advantageous as it minimizes information loss. This elucidates the rationale behind the removal of the final two residual stacks.

3.2.4 Methodology for Low SNR Classification Model (Transformer)

The Transformer model represents the advancement of the encoder-decoder design, as introduced in the paper "Attention is All You Need" (5). The encoder-decoder design traditionally utilizes recurrent neural networks (RNNs) for sequential information extraction, but the Transformer architecture does not employ RNNs. Transformer-based models have predominantly supplanted LSTM, demonstrating greater quality for numerous sequence-to-sequence tasks. We conduct research to identify the most recent and effective time-series model published. The initial way we are acquainted with is the typical approach utilizing recurrent neural networks (RNNs). RNNs function similarly to feed-forward neural networks, processing the input sequentially, one element at a time. The Encoder performs the unrolling of each symbol in the

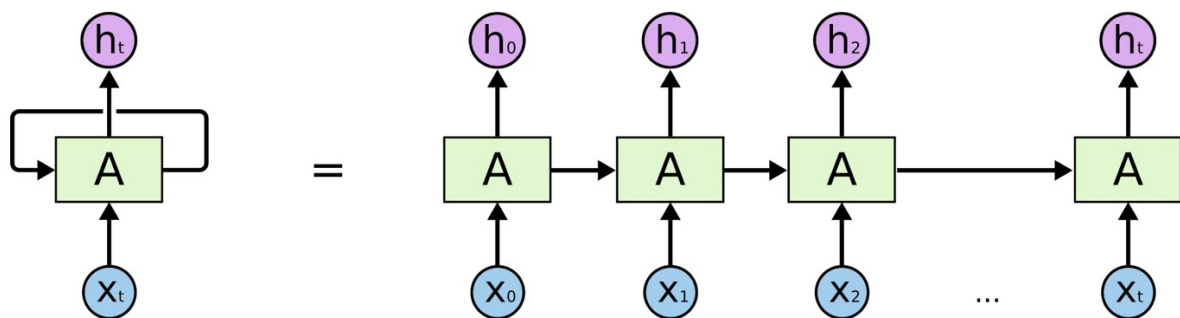


Figure 3.11: RNN working process

input, aiming to extract data from the sequential input and encode it into a vector, which serves as a representation of the input. Nonetheless, RNN models exhibit certain issues; they are difficult to train because of their reliance on sequential processing rather than parallelization, and they struggle with extended sequences because of the vanishing gradient problem. The second model, currently the most utilized in time-series analysis, is **Long-Short Term Memory (LSTM)** networks, specifically engineered to mitigate long-term reliance issues. Each LSTM cell permits historical information to bypass the current cell's processing and proceed to the subsequent cell, hence facilitating prolonged memory retention and enabling the unaltered flow of data. LSTM comprises an input gate that ascertains which new information to retain and a forget gate that dictates which information to discard.

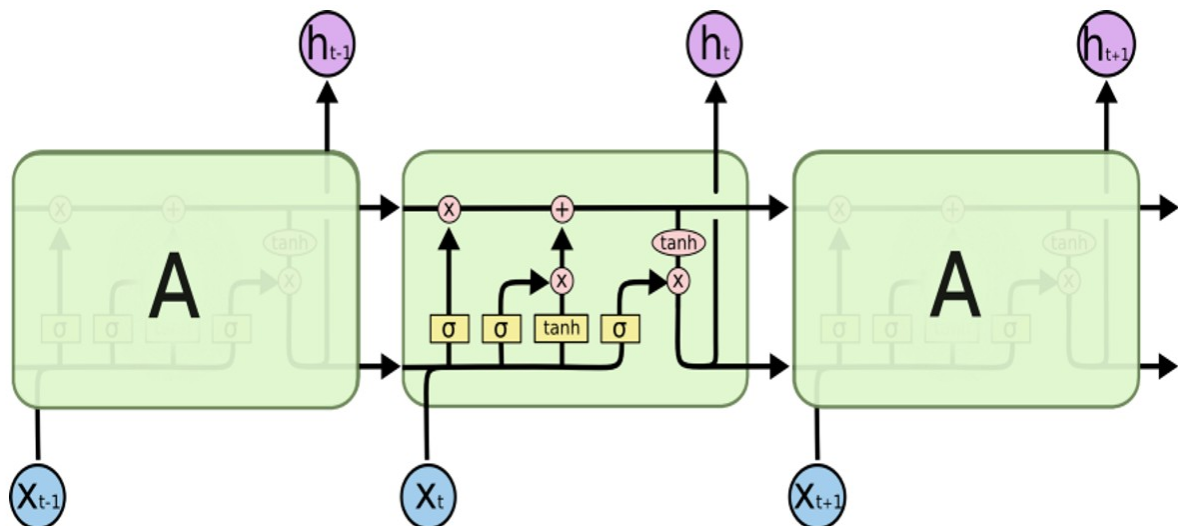


Figure 3.12: LSTM Structure

LSTMs provide enhanced memory capabilities, enabling them to manage longer sequences compared to RNNs. Nonetheless, LSTM networks exhibit greater sluggishness due to their increased complexity. A further limitation of an RNN-based encoder-decoder architecture is the fixed-length vector. Employing a fixed-length vector to represent the input sequence for decoding a completely new text is challenging. The context vector is incapable of retaining all the information when the input sequence is extensive. Moreover, it is difficult to distinguish phrases that contain identical words yet convey different meanings.

Subsequently, we devise a solution utilizing the latest state-of-the-art time series model known as Transformer. This approach offers advantages over earlier methods, including the utilization of parallel processing, thereby using contemporary graphics processing units (GPUs) optimized for parallel calculation. It addresses the vanishing gradient problem by allowing the input size to be of any dimension, enabling the network to process data concurrently rather than sequentially. The context of data is effectively represented by the utilization of positional encoding and the self-attention mechanism embedded into the network modules.

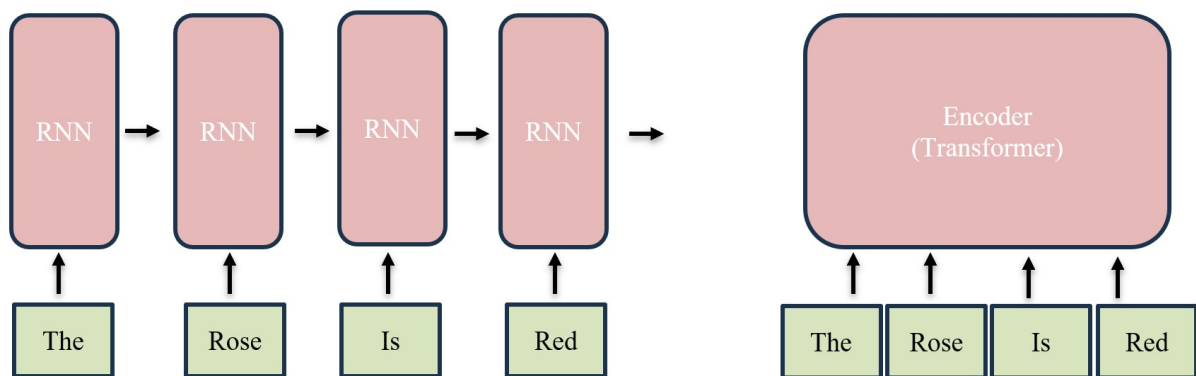


Figure 3.13: RNN Based Encoder and Transformer's Encoder

Proposed Transformer Architecture: We suggested a novel architecture designed exclusively for managing noisy signal modulation and low SNR signal modulation, as illustrated in the Table 3.3 below. We implement batch normalization to mitigate overfitting, alongside two fully connected networks and Alpha Dropout. Alpha dropout maintains the mean and variance values of inputs at their original levels, hence maintaining the self-normalizing property post-dropout phase. We employed the Scaled Exponential Linear Unit (SeLU) as the activation function to facilitate the self-normalizing property in conjunction with the dropout layer. We will continue to utilize Lazy Adam as the model optimizer, consistent with the improved ResNet. Every type of signal modulation has a different pattern of data, which we can classify using the transformer network and take advantage of its modules.

Table 3.3: Proposed Transformer Architecture (Optimizer: LazyAdam)

Layer	Output Dimension
Input	2×1024
Transformer Block Feed Forward: 256 nodes	2×1024
Global Average Pooling	1024
Batch Normalization	1024
Alpha Dropout (0.3)	1024
FC/SeLU-Alpha Dropout (0.2)	128
FC/SeLU-Alpha Dropout (0.2)	128
FC/Softmax	24

Chapter 4

Results

4.1 Radio Frequency Signal Sensing

Initially we connected the red pitaya directly to the RF source for testing if the device can capture signals generated at any certain frequency. The device successfully captured and plotted the captured signal, which was set at 40MHz as displayed in Fig 4.1 below.

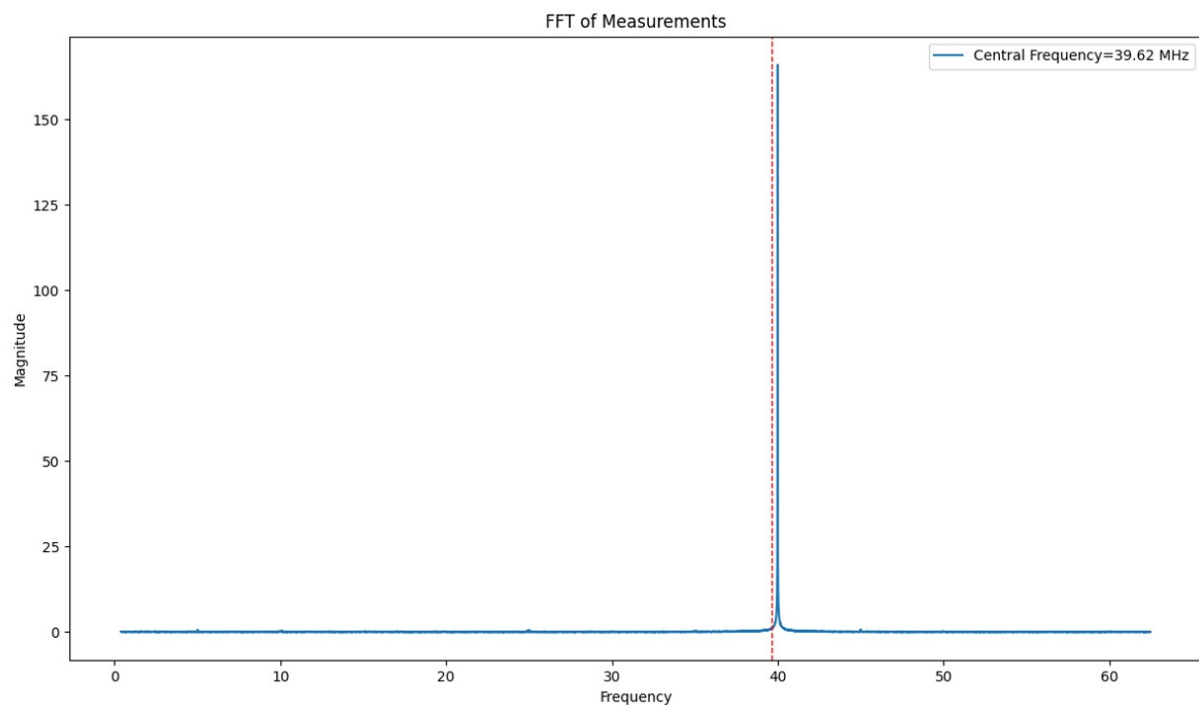


Figure 4.1: Synthetic Spectrum Plot for Signal Detection

The first prominent peak observed in the FFT spectrum is located at **39.62 MHz**, which closely aligns with the signal generated by our RF signal source configured at **40 MHz** with a transmission power level of **+5 dB**. This minor frequency offset (approximately 0.38 MHz) may be attributed to hardware imperfections such as oscillator drift, sampling jitter, or slight inaccuracies in the RF front-end calibration. Nevertheless, the detection of this peak confirms the successful capture of our intended test signal within the measured spectrum. The current

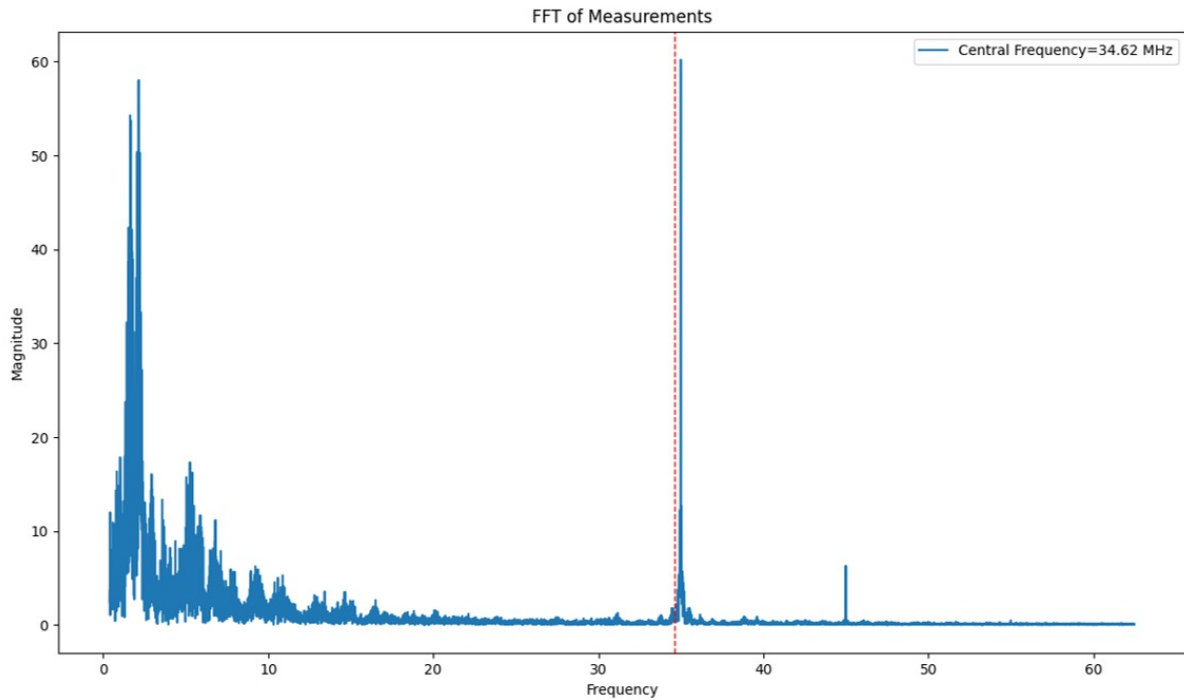


Figure 4.2: Observed Spectrum Plot for 40MHz RF emission

RF sensing model successfully detects and distinguishes **five distinct signal sources** within the specified observation window. Among these, **four peaks correspond to known, independently transmitted sources**, each located at different frequency positions and likely associated with intentional transmissions from controlled RF emitters. Additionally, **one prominent peak at the lower frequency range** appears to originate from an **unidentified or unexpected source**, labeled as an **Unknown Source** in the FFT plot. This ability to detect both known and unknown transmissions demonstrates the projects effectiveness in spectrum monitoring and interference analysis, highlighting its potential application in electronic surveillance, signal intelligence (SIGINT), and situational awareness in dynamic RF environments. The third

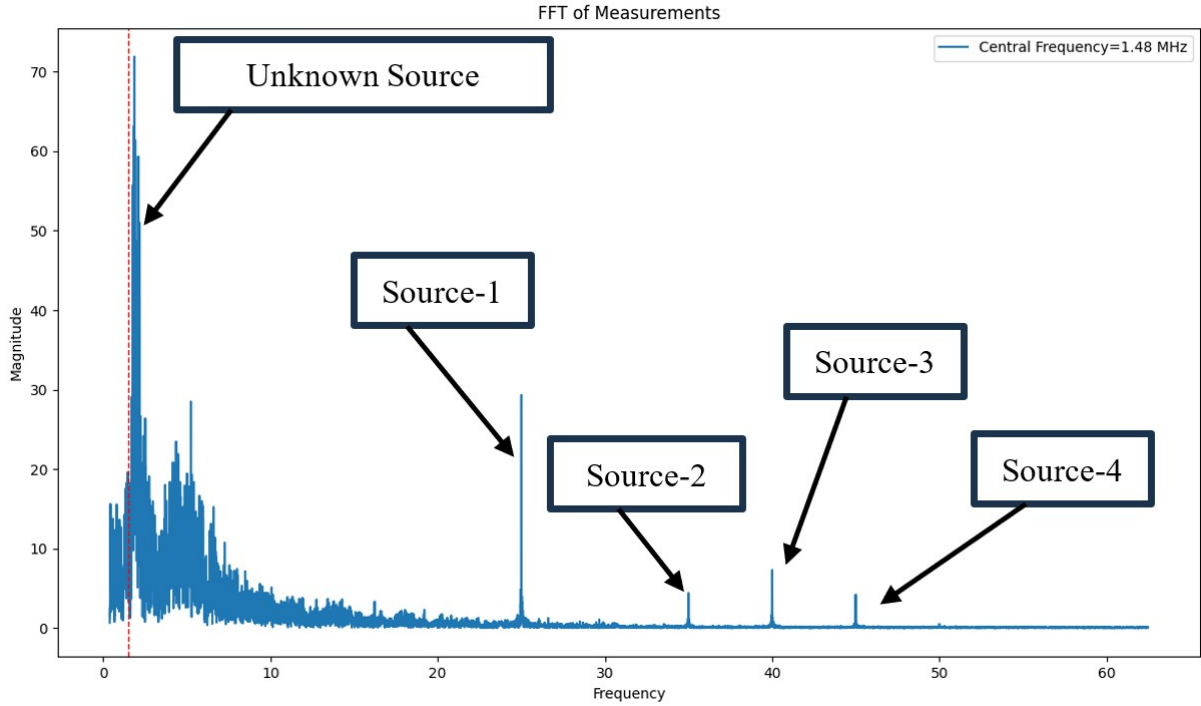


Figure 4.3: Observed Spectrum Plot for Multiple Simultaneous RF emissions

Table 4.1: RF Sources with their Frequencies and Transmission Amplitudes

RF Source	Frequency	Tx Amplitude
Source-1	25 MHz	+10dB
Source-2	35 MHz	+2dB
Source-3	40 MHz	+5dB
Source-4	45 MHz	+3dB
Unknown Source	1.48 MHz	>+10dB

prominent peak observed during our measurements falls within the **1.35 to 1.5 MHz** frequency range. Upon further analysis, we identified **potential sources of this RF emission** by referencing nearby high-power medium wave (MW) transmitters operated by **Prasar Bharti**. As shown in Table 4.2, probable candidates include transmitters located in **Bhopal (1593 kHz, 10 kW)**, **Gwalior (1386 kHz, 20 kW)**, and **Rewa (1179 kHz, 20 kW)**. Given the proximity of these locations to our testing site at **IIT Indore**, and the high transmission power of the signals, it is reasonable to infer that one of these stations could be contributing to the observed spectral activity in this band.

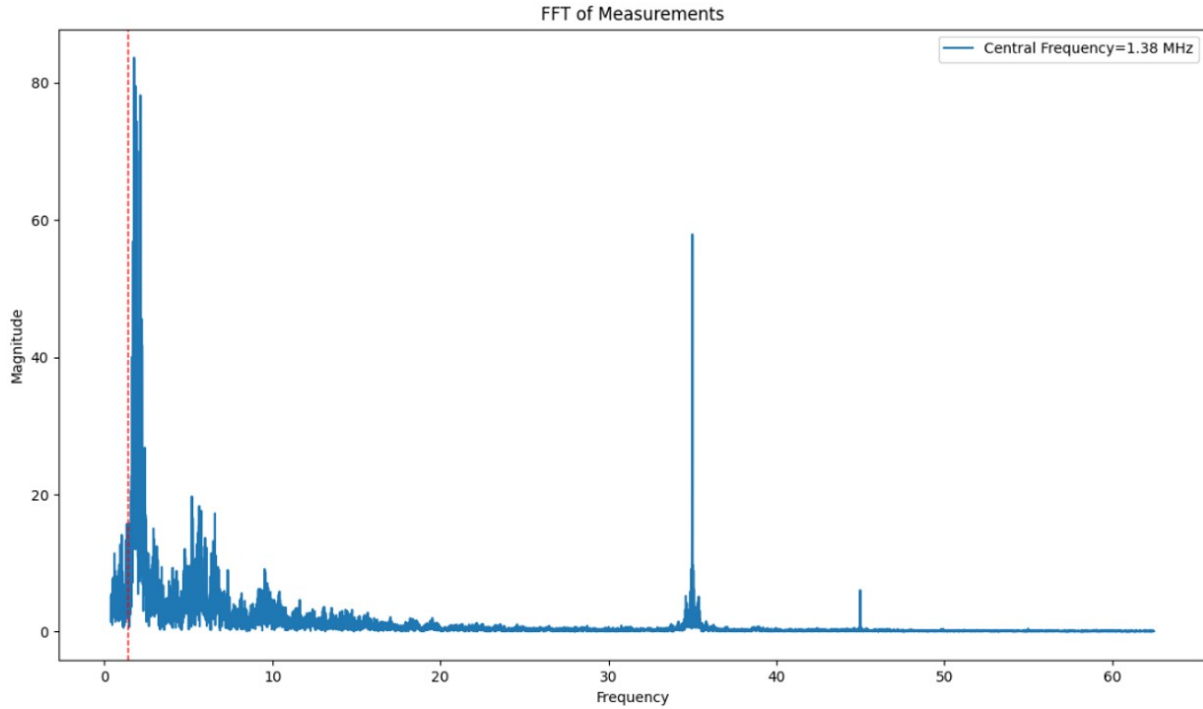


Figure 4.4: Observed Spectrum Plot for 1.38MHz Unknown RF emission

Table 4.2: Probable RF Emission Sources for Signal detected at 1.35 to 1.5 MHz

Location	Transmitter	Frequency
Bhopal	10 kW MW	1593 kHz
Gwalior	20 kW MW	1386 kHz
Rewa	20 kW MW	1179 kHz

Source: Prasar Bharti

4.2 Radio Frequency Modulation Classification

4.2.1 High SNR (Modified Residual Network)

The result shown in Fig. 4.3 illustrate a significant improvement in classification performance achieved by modifying the ResNet architecture. Specifically, the modified model was able to **increase the maximum accuracy from a baseline of 93.7% to an enhanced 95.9%**. This improvement is particularly notable in high SNR scenarios, where the signal is strong and noise levels are minimal, allowing the model to learn more distinguishable features.

The accuracy curve exhibits a steep rise as the SNR increases, reflecting the model's improved capability to distinguish relevant signal characteristics under cleaner input conditions.

The highlighted data points, especially at SNR levels of 18 dB and above, demonstrate the modified model's robustness and its ability to consistently maintain high accuracy across a wide range of favorable signal environments. This confirms that the enhancements made to the network architecture effectively boost the model's generalization and classification power in high SNR conditions.

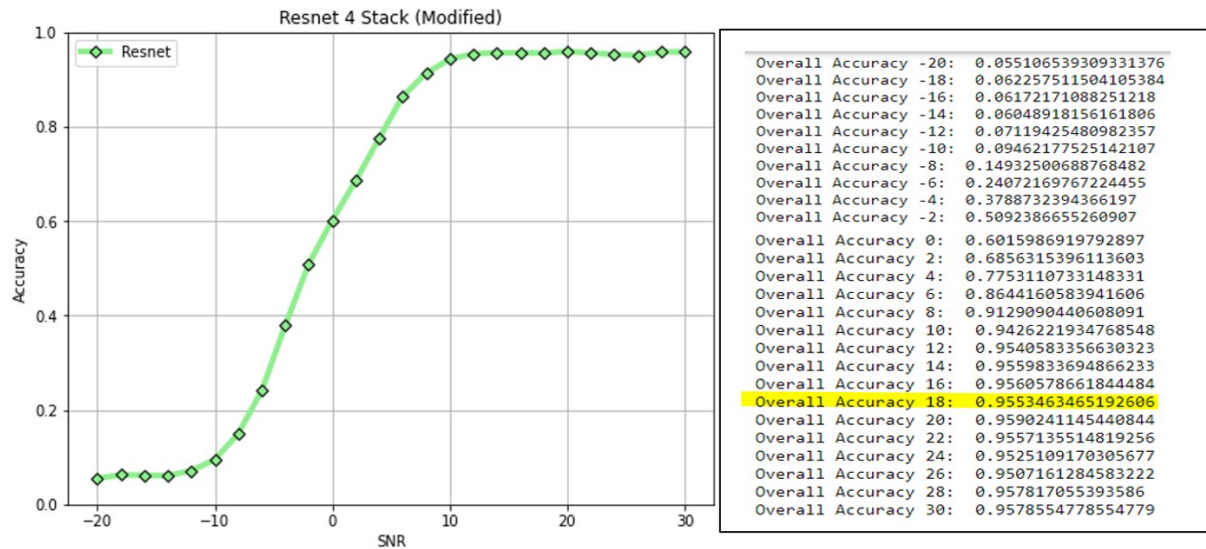


Figure 4.5: Result for High SNR Model

4.2.2 Low SNR (Transformer Network)

The results presented in the Fig.4.4 highlight the superior capability of the Transformer-based model in handling signal classification tasks under low Signal-to-Noise Ratio (SNR) conditions. Most notably, at an SNR of -8 dB, the model achieved an impressive accuracy of **72.6%**, which is significantly higher compared to the performance of the previously used ResNet model. The ResNet-based approach struggled to learn any meaningful features in extreme noise conditions and **achieved a maximum accuracy of only 20%** in the low SNR range between -20 dB to 0 dB—an accuracy level often considered equivalent to random guessing.

In contrast, the Transformer architecture demonstrates robustness in the presence of noise and is capable of identifying patterns and extracting signal features even when the signal is heavily buried in noise. This result strongly supports the effectiveness of the Transformer

model in challenging real-world environments, where low SNR conditions are common and signal detection is critical. Such performance improvement marks a substantial advancement in the reliability and practicality of RF sensing in noisy scenarios.

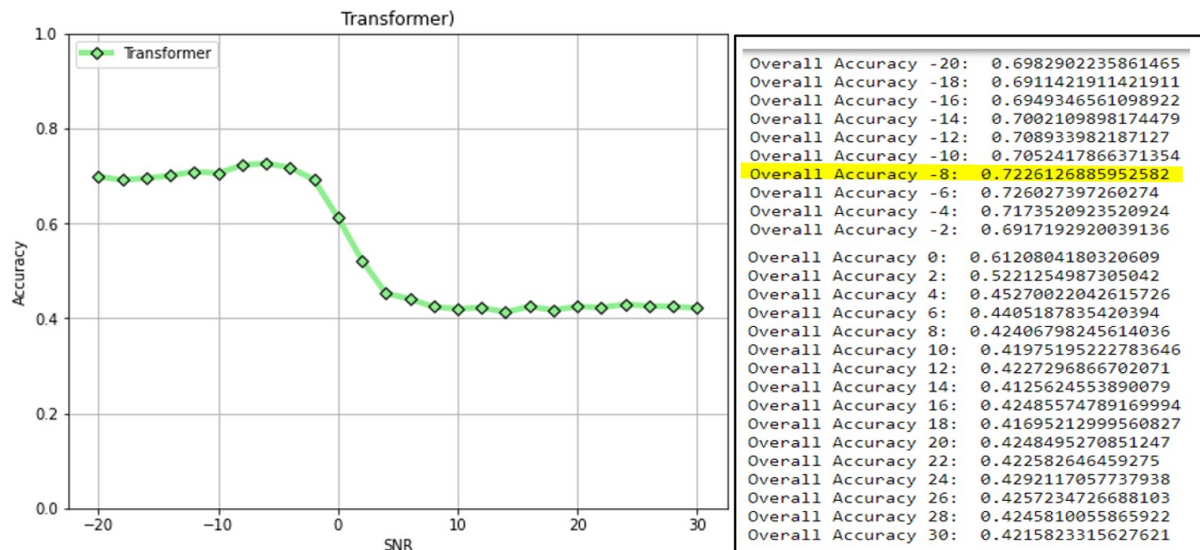


Figure 4.6: Result for Low SNR Model

4.2.3 Low SNR + High SNR (Ensembled Output from both Networks)

The results shown in the Fig.4.5 demonstrate the effectiveness of combining both Transformer and ResNet architectures into a single ensemble model. By leveraging the unique strengths of each network—ResNet’s strong feature extraction in high SNR conditions and the Transformer’s robustness to noise in low SNR environments—the ensemble approach achieves consistently high accuracy across the full SNR spectrum.

Specifically, in low SNR conditions such as -6 dB, the model attains an accuracy of **73.0%**, which surpasses the individual performance of both the standalone Transformer and ResNet models in this region. Simultaneously, in high SNR conditions such as 22 dB, the ensemble achieves a maximum accuracy of **95.6%**, maintaining the superior classification performance observed in the modified ResNet.

This balance in performance across varying noise levels confirms the ensemble’s adaptability and generalization capability. It effectively handles noisy, real-world environments while

also capitalizing on clearer signal conditions, making it a robust solution for RF signal classification in diverse operational scenarios.

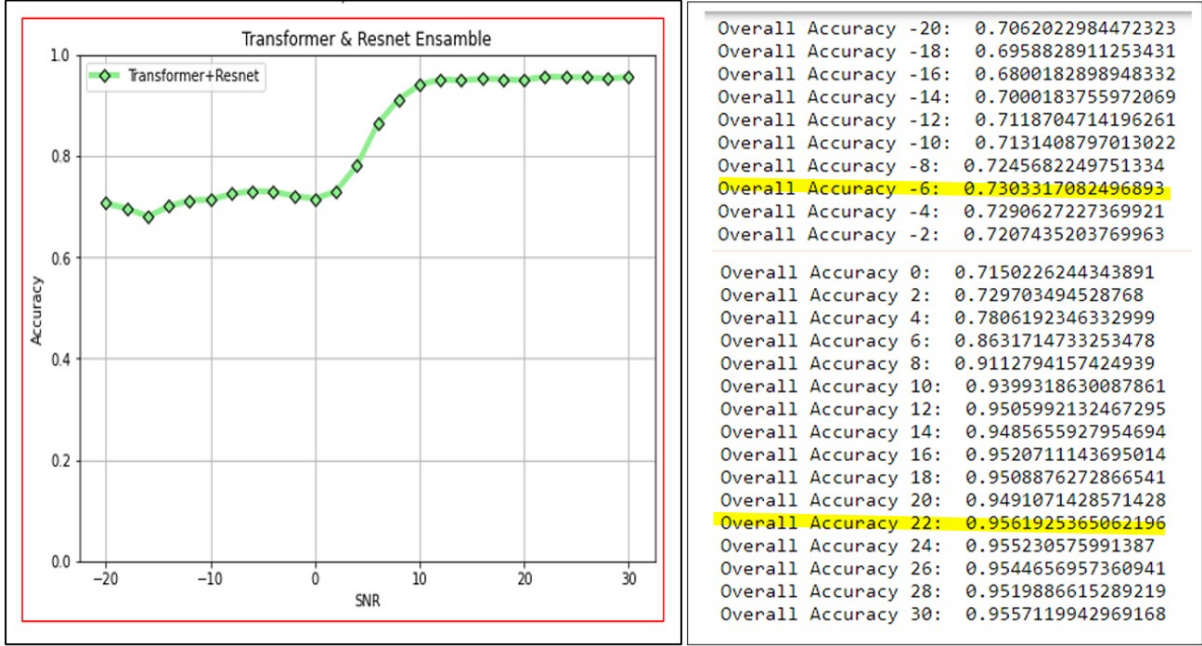


Figure 4.7: Ensembled Result of two Neural Networks

4.2.4 Comparison with Baseline ResNet Network

The experimental results illustrated in Fig.4.6 demonstrate the superior performance of the proposed models across varying SNR environments, highlighting the effectiveness of our architecture in both high and low signal quality conditions. In high SNR scenarios, where the signal is strong and minimally affected by noise, the **modified ResNet model achieved a maximum classification accuracy of 95%**, outperforming the **baseline ResNet model's 93.7%**. Furthermore, the **X-Vector model surpassed both, reaching an impressive 98%**, indicating its strong capability to leverage clear signal features.

More critically, in challenging low SNR conditions (SNR = -20 dB to 0 dB), where traditional models typically struggle, the performance gap becomes even more significant. The baseline ResNet model and X-Vector model were able to achieve only 14% and 17% accuracy, respectively—figures that approximate random guessing. In contrast, the **proposed Transformer model demonstrated remarkable robustness to noise, achieving an accuracy of**

70%, which marks a **substantial improvement of over 55 percentage points** compared to the baseline. This significant enhancement illustrates the Transformer's strength in learning relevant patterns even under severely degraded signal conditions.

Overall, these results validate the efficacy of our architectural enhancements, particularly the use of Transformer networks for low SNR environments and modified ResNet for high SNR environments. The models' complementary strengths further support the potential of ensemble approaches for achieving high accuracy and robustness across diverse and unpredictable RF environments.

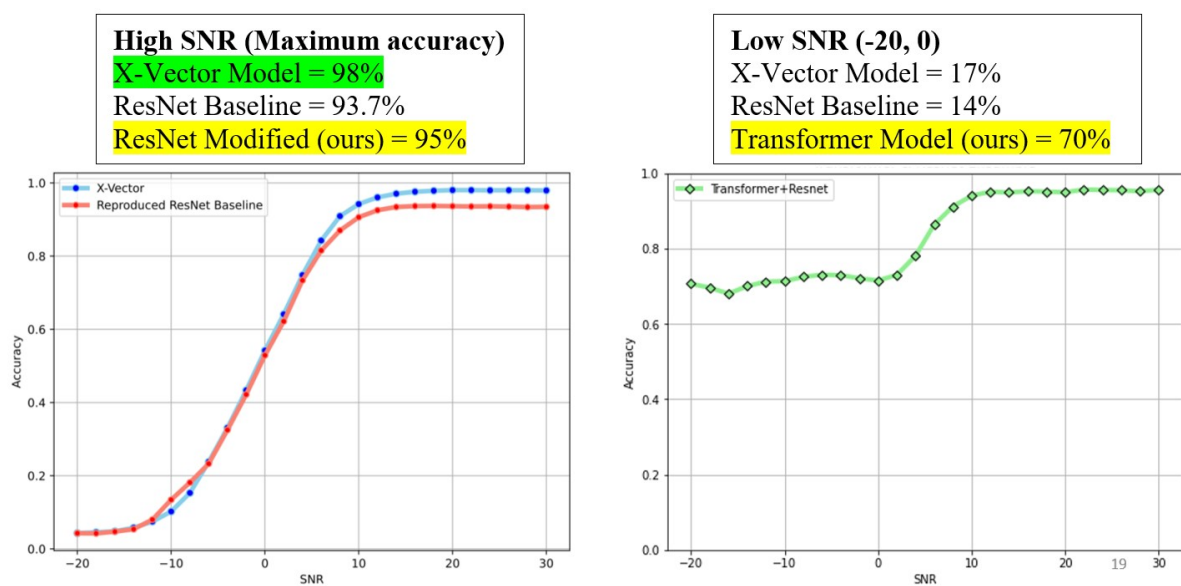


Figure 4.8: Comparison with Baseline ResNet Network

Chapter 5

Project Conclusion

In this project, we developed a robust and portable RF sensing system capable of accurately detecting and classifying signals across a wide range of Signal-to-Noise Ratios (SNRs). By integrating the Donut Wideband Antenna, a low-noise transimpedance amplifier, Red Pitaya STEMLab 125-10, and Raspberry Pi 3B+, we established a complete hardware-software pipeline for real-time signal acquisition and processing.

On the algorithmic side, we explored multiple neural network architectures—including ResNet, Transformer, and X-Vector models—evaluating their performance in both high and low SNR conditions. Our **modified ResNet model improved high SNR classification accuracy from 93.7% to 95%**, while the **Transformer model achieved a significant jump from 14% to 70% in low SNR conditions**. Further, the ensemble of ResNet and Transformer networks demonstrated balanced and reliable performance across the full SNR spectrum.

The combined hardware-software framework and deep learning models developed in this work not only enhance RF signal recognition in varied noise environments but also lay a strong foundation for future extensions in intelligent wireless sensing, surveillance, and spectrum monitoring applications.

Chapter 6

Future Work

The promising results obtained from our current RF sensing system—demonstrating strong performance across both high and low SNR environments—lay a solid foundation for future enhancements and real-world deployment. One of the primary extensions of this work involves **deploying the RF sensing unit on a drone platform**. This mobile deployment will enable **real-time signal monitoring across broader geographical regions**, especially in dynamic environments where the electromagnetic landscape continuously changes.

A major focus of the next phase will be on **SNR estimation from the data captured by the Red Pitaya-based RF sensing unit mounted on the drone**. Instead of relying on synthetic or pre-labeled datasets, we aim to generate a **custom RF dataset** from real-world scenarios. The SNR estimation process will involve measuring the power of the desired signal relative to background noise within specific time-frequency windows. This will require the application of signal processing techniques such as spectral subtraction, noise floor estimation, and signal averaging to reliably separate and quantify signal and noise components. These estimations will help us label data more accurately, enabling more refined training and evaluation of deep learning models in authentic operational conditions.

Given that data collection and labeling is a time-intensive task, we will concurrently focus on optimizing the system for **deployment on a low-power FPGA platform, such as the Xilinx ZCU104**. This will allow for **real-time model inference at the edge**, making the system

suitable for embedded and power-constrained environments, such as aerial drones or remote surveillance units.

The final and most strategic direction of this work will align with **Electronic Support Measures (ESM)**. In this context, our system will be tailored for **RF signal search, detection, classification, and threat analysis**—key capabilities in defense and surveillance applications. By analyzing the electromagnetic emissions intercepted in the environment, the system can help **identify hostile or unknown transmissions**, assess their potential threat level, and support **military decision-making protocols**. This transition from lab-scale experimentation to mission-oriented applications represents a critical step toward realizing a fully autonomous, intelligent RF sensing solution.

Bibliography

- [1] T. J. O'Shea, T. Roy, and T. C. Clancy, "Over-the-air deep learning-based radio signal classification," *IEEE J. Sel. Topics Signal Process.*, vol. 12, no. 1, pp. 168–179, 2018, doi:10.1109/JSTSP.2018.2797022.
- [2] C. A. Harper *et al.*, "Enhanced automatic modulation classification using deep convolutional latent space pooling," in *Proc. Asilomar Conf. Signals, Syst., Comput.*, 2020.
- [3] A. J. Uppal, M. Hegarty, W. Haftel, P. A. Sallee, H. Brown Cribbs, and H. H. Huang, "High-performance deep learning classification for radio signals," in *Proc. 53rd Asilomar Conf. Signals, Syst., Comput.*, Pacific Grove, CA, USA, 2019, pp. 1026–1029, doi:10.1109/IEEECONF44664.2019.9048897.
- [4] S. Huang *et al.*, "Automatic modulation classification using compressive convolutional neural network," *IEEE Access*, vol. 7, pp. 79636–79643, 2019, doi:10.1109/ACCESS.2019.2921988.
- [5] A. Vaswani, N. Shazeer, N. Parmar, J. Uszkoreit, L. Jones, A. N. Gomez, Ł. Kaiser, and I. Polosukhin, "Attention is all you need," in *Adv. Neural Inf. Process. Syst.*, 2017, pp. 5998–6008.
- [6] T. J. O'Shea, J. Corgan, and T. C. Clancy, "Convolutional radio modulation recognition networks," in *Eng. Appl. Neural Netw.*, Springer, 2016, pp. 213–226.
- [7] G. Klambauer, T. Unterthiner, A. Mayr, and S. Hochreiter, "Self-normalizing neural networks," *arXiv preprint arXiv:1706.02515*, 2017.

- [8] T. O'Shea and J. Hoydis, "An introduction to deep learning for the physical layer," *IEEE Trans. Cogn. Commun. Netw.*, 2017.
- [9] K. Z. Haigh and J. Andrusenko, *Cognitive Electronic Warfare: An Artificial Intelligence Approach*. Norwood, MA, USA: Artech House, 2021.
- [10] T. O'Shea and N. West, "Radio machine learning dataset generation with GNU Radio," *Proc. GNU Radio Conf.*, vol. 1, no. 1, 2016.
- [11] T. O'Shea, J. Corgan, and T. C. Clancy, "Convolutional radio modulation recognition networks," in *Eng. Appl. Neural Netw.*, Springer, 2016, pp. 213–226, doi:10.1007/978-3-319-44188-7_16.
- [12] P. Wu, B. Sun, S. Su, J. Wei, J. Zhao, and X. Wen, "Automatic modulation classification based on deep learning for software-defined radio," *Math. Probl. Eng.*, vol. 2020, Art. no. 2678310, 2020.
- [13] D. L. Adamy, *EW 105: Space Electronic Warfare*. Norwood, MA, USA: Artech House, 2021.
- [14] A. K. Nandi and E. E. Azzouz, "Algorithms for automatic modulation recognition of communication signals," *IEEE Trans. Commun.*, vol. 46, no. 4, pp. 431–436, 1998.
- [15] D. Kingma and J. Ba, "Adam: A method for stochastic optimization," *arXiv preprint arXiv:1412.6980*, 2014.